Jefferson Lab PAC14
Proposal Cover Sheet

This document must be received by close of business Thursday, **June 4, 1998** at:

Jefferson Lab
User Liaison Office,
Mail Stop 12B
12000 Jefferson Avenue
Newport News, VA
23606

Experimental Hall: A

Days Requested for Approval: 14

☒ **New Proposal Title:** A MEASUREMENT OF DISPERSING EFFECTS IN THE ELASTIC AND INELASTIC SCATTERING OF ELECTRONS FROM POLARIZED ^{3}HE

☐ **Update Experiment Number:**

☐ **Letter-of-Intent Title:**

(Choose one)

Proposal Physics Goals

Indicate any experiments that have physics goals similar to those in your proposal.

Approved, Conditionally Approved, and/or Deferred Experiment(s) or proposals:

—

Contact Person

Name: KETEVI ASSAMAGAN
Institution: HAMPTON UNIVERSITY
Address: PHYSICS DEPARTMENT
Address: HAMPTON UNIVERSITY
City, State, ZIP/Country: HAMPTON, VA 23668
Phone: (757) 269 7167 **Fax:** (757) 269 7363
E-Mail: KETEVI@JLAB.ORG

Jefferson Lab Use Only

Receipt Date: 6/4/98 PR98-[redacted]102

By: [redacted]

BEAM REQUIREMENTS LIST

JLab Proposal No.: 98-102 Date: 06-04-98

Hall: A Anticipated Run Date: _____ PAC Approved Days: _____

Spokesperson: JOE MITCHELL Hall Liaison: J P. Chen
Phone: 269 7851
E-mail: MITCHELL@JLAB.ORG

List all combinations of anticipated targets and beam conditions required to execute the experiment. (This list will form the primary basis for the Radiation Safety Assesment Document (RSAD) calculations that must be performed for each experiment.)

Condition No.	Beam Energy (MeV)	Mean Beam Current (μA)	Polarization and Other Special Requirements (e.g., time structure)	Target Material (use multiple rows for complex targets — e.g., w/windows)	Material Thickness (mg/cm²)	Est. Beam-On Time for Cond. No. (hours)
1	845	15	–	^{3}He w.	50	144
				glass windows	50	
2	845	15	–	glass windows	50	24
3	1645	15	–	^{3}He w.	50	144
				glass windows	50	
4	1645	15	–	glass windows	50	24

The beam energies, E_{Beam}, available are: $E_{Beam} = N \times E_{Linac}$ where N = 1, 2, 3, 4, or 5. E_{Linac} = 800 MeV, i.e., available E_{Beam} are 800, 1600, 2400, 3200, and 4000 MeV. Other energies should be arranged with the Hall Leader before listing.

LAB RESOURCES LIST

JLab Proposal No.: 98-102 Date 06-04-98

(For JLab ULO use only.)

List below significant resources — both equipment and human — that you are requesting from Jefferson Lab in support of mounting and executing the proposed experiment. Do not include items that will be routinely supplied to all running experiments such as the base equipment for the hall and technical support for routine operation, installation, and maintenance.

Major Installations *(either your equip. or new equip. requested from JLab)*

POLARIZED ^{3}HE TARGET

FOCAL PLANE HODOSCOPE

New Support Structures:

Data Acquisition/Reduction

Computing Resources:

STANDARD

New Software:

Major Equipment

Magnets: —

Power Supplies: —

Targets: —

Detectors: —

Electronics: —

Computer Hardware: —

Other: —

Other: —

HAZARD IDENTIFICATION CHECKLIST

JLab Proposal No.: 98-102 (For CEBAF User Liaison Office use only.) Date: 06-04-98

Check all items for which there is an anticipated need.

Cryogenics
- ____ beamline magnets
- ____ analysis magnets
- ____ target
  - type: ____
  - flow rate: ____
  - capacity: ____

Electrical Equipment
- ____ cryo/electrical devices
- ____ capacitor banks
- ____ high voltage
- ____ exposed equipment

Radioactive/Hazardous Materials
List any radioactive or hazadorous/ toxic materials planned for use:
NONE

Pressure Vessels
- ____ inside diameter
- ____ operating pressure
- ____ window material
- ____ window thickness

Flammable Gas or Liquids
- type: ____
- flow rate: ____
- capacity: ____

Drift Chambers HRS
- type: STANDARD
- flow rate: ____
- capacity: ____

Other Target Materials
- ___ Beryllium (Be)
- ___ Lithium (Li)
- ___ Mercury (Hg)
- ___ Lead (Pb)
- ___ Tungsten (W)
- ___ Uranium (U)
- X Other (list below)
  ^{3}He gas, Rb, N_2, H_2 gas

Vacuum Vessels
- ____ inside diameter
- ____ operating pressure
- ____ window material
- ____ window thickness

Radioactive Sources
- ____ permanent installation
- ____ temporary use
- type: ____
- strength: ____

NONE

Large Mech. Structure/System
- ____ lifting devices
- ____ motion controllers
- ____ scaffolding or
- ____ elevated platforms

NONE

Lasers
- type: DIODE LASER
- wattage: ~ 100W
- class: IV

Installation:
- X permanent
- ____ temporary

(for experiment)

Use:
- ____ calibration
- ____ alignment

for ^{3}He target

Hazardous Materials
- ___ cyanide plating materials
- ___ scintillation oil (from)
- ___ PCBs
- ___ methane
- ___ TMAE
- ___ TEA
- ___ photographic developers
- ___ other (list below)

General:

Experiment Class:
- ____ Base Equipment
- ✓ Temp. Mod. to Base Equip.
- ____ Permanent Mod. to Base Equipment
- ____ Major New Apparatus

Other: ____

A Measurement of Dispersive Effects in the Elastic and Inelastic Scattering of Electrons from Polarized ^{3}He

K.A. Assamagan (Spokesperson), O.K. Baker, W. Buck, L. Gan,
A. Gasparian, P. Gueye, C.E. Keppel, L. Tang
Hampton University

H. Anklin, R. Carlini, J.A. Dunne, R. Ent (Spokesperson),
J-O. Hansen, K. De Jager, C. Keith, M. Liang, A. Lung, D. Mack,
J.H. Mitchell (Spokesperson), A. Saha, B. Wojtsekhowski,
W.F. Vulcan
Jefferson Lab

S. Choi, S. Inerti, Z-E. Meziani
Temple University

W. Korsch
University of Kentucky

June 4, 1998

Abstract

The planned experiment will measure the target asymmetry in the elastic and inelastic scattering of unpolarized electrons from a polarized target whose polarization axis is oriented normal to the scattering plane. In the case of elastic scattering such an asymmetry can only be due to dispersive corrections to the one-photon exchange amplitude. In the excitation of inelastic states such an amplitude could arise from either multi-photon exchange or the violation of time reversal invariance.

1 Introduction

The scattering of high energy electrons is normally pictured in the one-photon exchange approximation (first Born approximation). This is just the first term in the expansion of the full scattering amplitude in powers of the QED coupling constant, α. Some higher order effects are commonly accounted for, i.e., the radiative corrections and the Coulomb distortions. The radiative corrections include both pre and post bremsstrahlung and corrections to the propagator and vertices. The Coulomb distortions are treated approximately by an effective momentum transfer prescription or more exactly via the distorted wave Born approximation, DWBA. These Coulomb corrections to the cross section correspond to multiple photon exchanges with the target propagating in its ground state between successive exchanges, and the DWBA can be used to sum the effect of this class of multi-photon processes to all orders.

The dispersive term, which corresponds to the exchange of two photons with the target propagating between exchanges in an excited state, is usually neglected. As the intermediate state is not observable, the amplitude contains a sum over the excitation spectrum of the target and is therefore sensitive to the dynamics of the target system. This sum over the excited states of the target is reminiscent of the situation in real and virtual Compton scattering.

Several experimental techniques have been employed in the search for experimental signatures of the dispersive term. These are:

1. Examining the energy dependence of the elastic electron scattering cross section in the vicinity of a diffractive minimum.

2. Comparing the scattering of electrons and positrons.

3. Comparing charge radii deduced from electron scattering with those obtained from other techniques such as muonic atoms or in the case of the deuteron from the examination of atomic transition energies.

4. Searching for the inelastic excitation of a magnetic monopole transition.

5. Looking for a target asymmetry in the scattering of unpolarized electrons from a polarized spin $\frac{1}{2}$ target that has its polarization oriented normal to the electron scattering plane. For elastic scattering this is

equivalent to searching for a normal component of the polarization in the recoiling target.

The first technique requires a spin zero target so that only a C0 form factor can contribute and hence clear diffraction minima can be observed. Near diffraction minima the single photon exchange term is vanishing and the importance of higher order diagrams are relatively greater. It is advantageous to use light nuclei as the dispersive amplitude is roughly proportional to α while the Coulomb correction is proportional to αZ. For these reasons, and due to its ease of use, ^{12}C has been the traditional target of choice for these studies.

The second technique relies on the fact that the interference between the higher order corrections and the first order Born term changes sign for the scattering of positrons relative to electrons. Measurements have been made using ^{12}C, ^{208}Pb and the proton as targets. In the latter case, elastic, inelastic and deep-inelastic scattering have been examined. For nuclear targets, this technique also allows a careful check of the Coulomb corrections. The effective momentum transfer for electrons is higher than that for positrons and hence the positions of diffractive minima are slightly different in e^+ and e^- scatterings. This shift leads to very large effects in the ratio of the cross sections near minima.

The rms charge radii extracted from electron scattering and muonic atom studies tend to disagree, with the muonic result being larger. This discrepancy has been understood in terms of dispersive corrections to the electron scattering data [Off-91].

Selection rules for one photon exchange forbid the direct excitation of a magnetic monopole transition. The classic example would be $0^+ \rightarrow 0^-$. Since these transitions are forbidden in first order any observed strength would have to come from a two-step process such as dispersion.

The polarized target technique has been tried in both elastic and inelastic scattering from the proton. The recoil polarization technique has also been applied for electron-proton, (e-p), elastic scattering. In addition to experiments on the proton an attempt has been made to observe a normal component of the recoil polarization in elastic e-d scattering [Pre-68].

2 Current Experimental Situation

There have been many previous attemps to make quantitative measurements of dipersive effects in both complex nuclear systems and the nucleon. With essentially one exception these measurements have not had sufficient sensitivity to measure an unambiguous signal

and no signal has been observed in a system which is ameniable to reliable theoretical calculation.

The clearest measurements of dispersive effects are from the energy dependence of the ^{12}C elastic form factor [Off-91]. Low energy, $E_0 < 245$ MeV, elastic scattering data from IKO, NBS, Mainz and NIKHEF were used to determine a best fit charge distribution. This charge distribution was then used to predict the behavior of higher energy measurements of the cross section. The Born and Coulomb amplitudes are both uniquely determined by this static charge distribution.

Near the minimum of the cross section, $q = 1.85$ fm^{-1}, large deviations were found between the measured high energy cross sections and the predictions from the static charge distribution. These deviations are quantified by the percentage difference between the measured high energy cross section which contains both static and dynamic contributions and the prediction from the static charge distribution, $(\sigma_{disp+stat} - \sigma_{stat})/\sigma_{stat}$. The deviations near the minimum appear to grow linearly with beam energy and approach 18% for $E_0 = 690$ MeV. Figure 1 shows the measured energy dependence of the deviation in the vicinity of the first minimum [Off-91].

The static cross section in the minimum is largely determined by the imaginary part of the Coulomb amplitude as the Born term and the real part of the Coulomb amplitude are both zero at the diffractive minimum. The dominant dynamic contribution is thus the interference of the imaginary part of the Coulomb amplitude with the imaginary part of the dispersive term.

Outside of the region of the diffractive minimum, effects seem to be small, less than 2%, and vary smoothly with energy. In fact, the measurement of the dispersive term in this technique is relative to its size at the energy used to determine the static charge distribution, as any smoothly varying dispersive contribution will be absorbed into the fitted static charge distribution.

Theoretical calculations by Friar and Rosen predict an effect almost an order of magnitude smaller than is observed experimentally [FrR-74]. This would indicate that the calculation greatly underestimates the imaginary dispersive amplitude. They also fail to predict the observed, almost linear, energy dependence. There is also some evidence that the calculations underpredict the real part of the dispersive amplitude.

The ratio, R, of electron to positron scattering has been measured by many

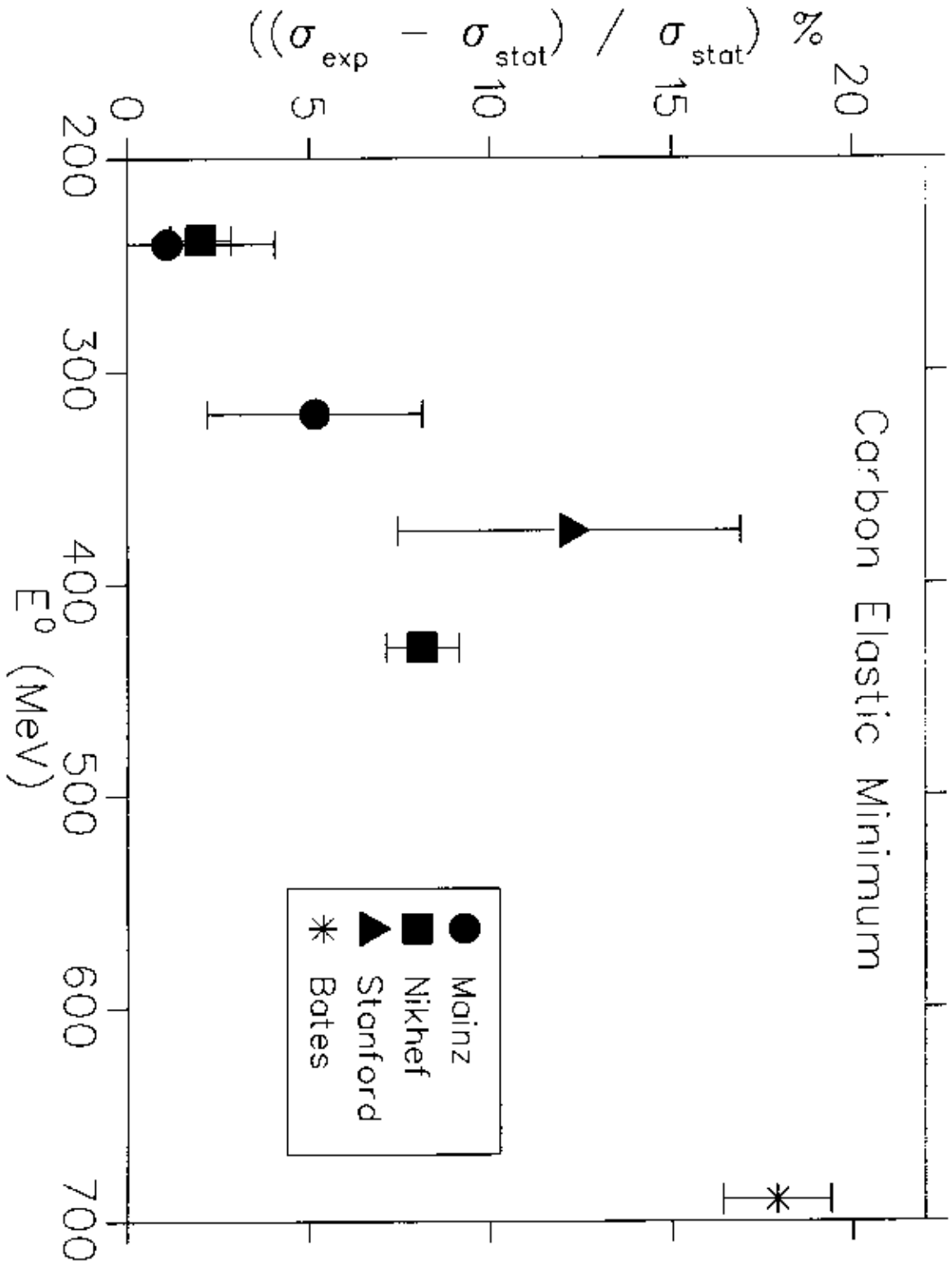

Figure 1: The observed deviation of the elastic carbon cross section from that predicted by the static charge distribution in the vicinity of the first form factor minimum.

groups [Bre-91], [Fan-76], [Roc-76], [Jos-74], [Mar-68], [Boq-68], [And-68], [Cas-67], [Bar-67], [Bro-64], [You-62]. For the proton, where Coulomb effects are small, this ratio is approximately given by $R \approx 1 + 4Re(M_2/M_1)$ where M_1 is the Born amplitude and M_2 is the two-photon exchange piece which includes both the second Born term and dispersion. It has been measured in elastic and inelastic kinematics at momentum transfers ranging from 0.005 to 14.9 $(\mathrm{GeV/c})^2$. The modern measurements claim error bars on R of 0.3% in inelastic kinematics [Fan-76]. All of these measurements are consistent with no dispersive contribution, $R = 1$. Naively, one would estimate that M_2/M_1 is of order α and hence one expects $(R - 1)$ to be ≈ 0.03. Indeed, early estimates using a simple model for the contribution of the resonances to the dispersive sum predict that the second order contributions change the electron scattering cross section by about 1% for elastic scattering at beam energies of a few GeV [Dre-58]. Thus the proton data indicate a smaller dispersive effect than one would guess from these simple estimates. Figure 2 shows the results of some of the world's R measurements.

Measurements of R in electron nucleus scattering are also sensitive to the real part of the dispersive amplitude, and in addition, allow a sensitive test of the Coulomb corrections. The Coulomb effects on R near diffractive minima in scattering from a heavy nucleus can be quite large. Indeed measurements of R using ^{208}Pb as a target find values approaching 3. While these data represent a demanding test of Coulomb corrections they do not place stringent limits on the size of the dispersive amplitude. In both lead and carbon all one can conclude from these results is that the dynamic effects are only a few percent of the cross section [Bre-91].

The observed discrepancies between the rms charge radius of the deuteron derived from atomic measurements [Sch-93], [Pac-94] and the same quantity extracted from electron scattering data has received a lot of attention in recent years [Kla-86],[Sic-96]. The discrepancy has largely been resolved by careful treatment of the Coulomb corrections to the electron scattering data but as a by product of this effort new calculations of the dispersive contributions to e-d elastic scattering have become available [Her-97]. Herrmann and Rosenfelder calculated the contributions of the virtual longitudinal excitations by numerically integrating a generalized structure function $S(q_1,q_2,\omega)$ derived from a separable form of the NN potential. For modest momentum transfers, a few fm^{-2}, and relatively low beam energies, a few hundred MeV, they find relative corrections due to the real part of the virtual longitudinal

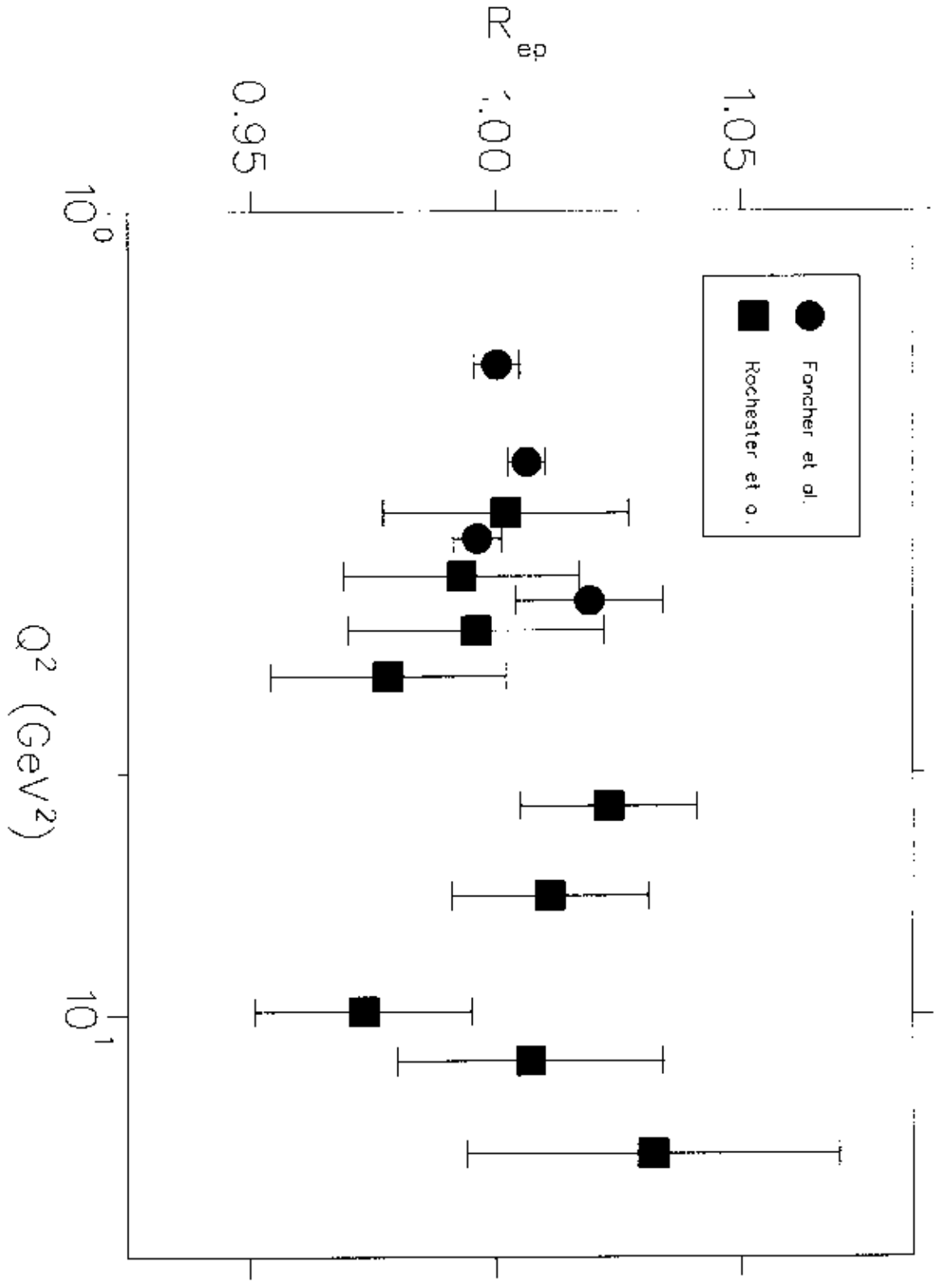

Figure 2: A sample of the world's measurements of the ratio of electron and positron cross sections on the proton.

excitations of order 10^{-3}. They also find that the correction to the rms radius of deuterium due to dispersion is about one third the size of that due to the Coulomb diagrams. The results of the calculations are shown in Figure 3.

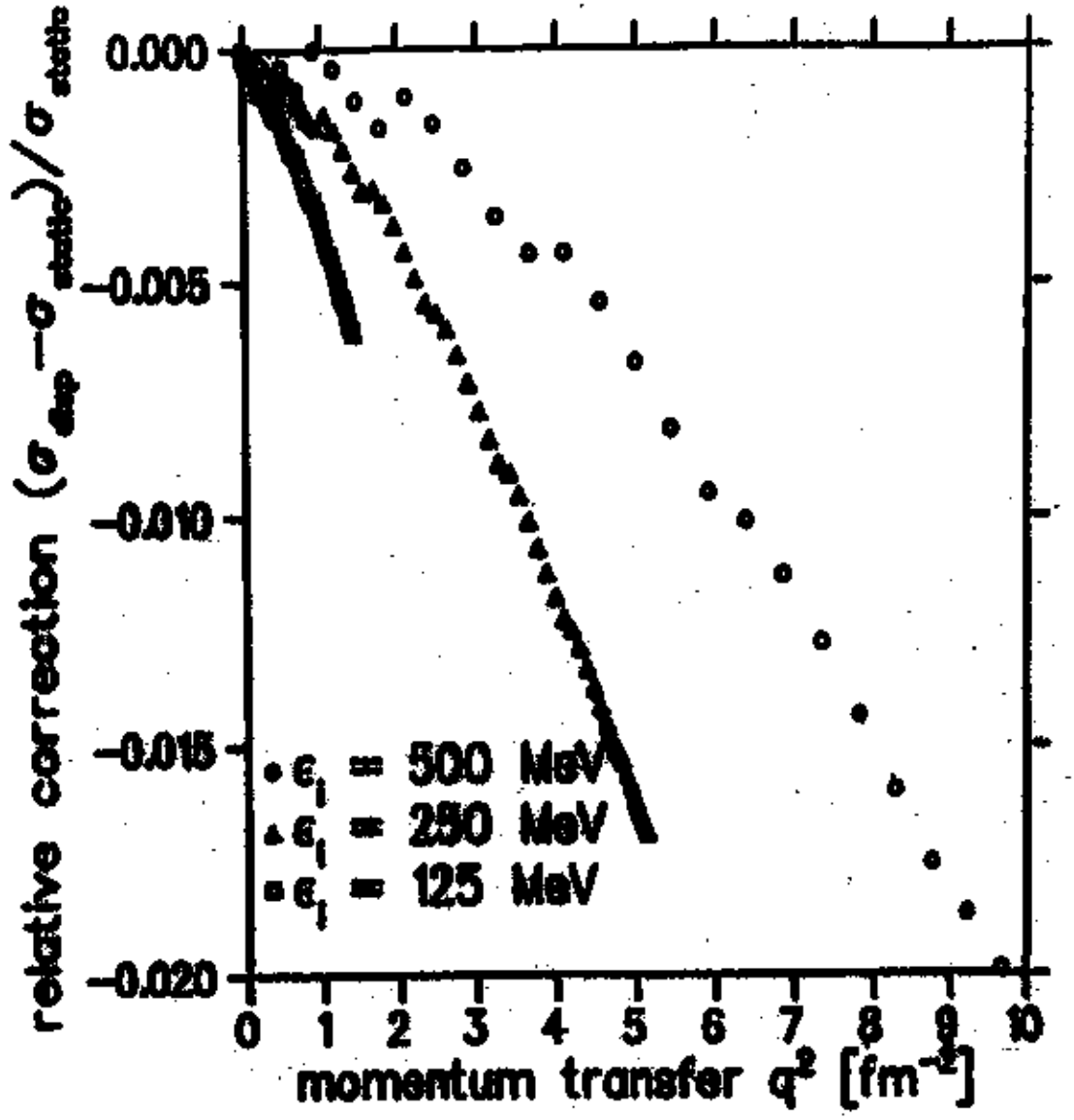

Figure 3: Calculations by Herrmann and Rosenfelder for the dispersive corrections to the elastic e-d scattering cross section.

There is only one reported cross section for the excitation of a monopole transition [Voe-91]. They measured a cross section of $5.4 \pm 3.8 * 10^{-37}$ cm^{-2}/sr for scattering to the 0^- state at E_x=10.957 MeV in ^{16}O. While the magnitude of the measured cross section agrees

with theoretical calculations by Borie and Drechsel [Bor-71] the statistical and systematic uncertainties of the result are not adequate to test any of the model assumptions and any substantial reduction of the experimental uncertainties would require a major effort [Voe-91]. The results from such a measurement are sensitive to the magnitude of the dispersive amplitude and hence would give information on both the real and imaginary parts of the amplitude if sufficient accuracy could be obtained.

Several attempts have been made to measure a nonzero normal recoil polarization in elastic electron-proton scattering [Lun-68], [DiG-65], [Biz-65]. The group from Orsay reported $P_n = 0.04 \pm 0.027$ and $P_t = 0.00 \pm 0.028$ and thus saw a signal for P_n at the one sigma level [Biz-65]. The transverse polarization is parity forbidden for an unpolarized electron beam and thus serves as a check of the systematics. The measurement was taken at a beam energy of 950 MeV and a Q^2 of 0.59 $(\mathrm{GeV/c})^2$. Two other measurements of this quantity gave answers which were consistent with zero. Stanford obtained $P_n = 0.013 \pm 0.02$ with a 900 MeV incident beam and a momentum transfer of 0.39 $(\mathrm{GeV/c})^2$ [Lun-68]. The other published measurement reports $P_n = 0.024 \pm 0.050$ at a momentum transfer of 0.78 $(\mathrm{GeV/c})^2$ and $E_0 = 900$ MeV from Frascati [DiG-65]. It would be hard to push this technique far below the 0.5% level as false asymmetries become increasingly difficult to control.

Prepost et al. reported a value of $P_n = 0.075 \pm 0.088$ for the normal vector polarization in elastic e-d scattering [Pre-68]. This was intended to test the time reversal invariance of the electromagnetic interaction but an elastic asymmetry measurement from a spin-1 system would be sensitive to two photon contributions.

Two polarized target measurements have been performed at SLAC. Powell et al. found no target asymmetry in the elastic scattering of unpolarized electrons from a proton target whose polarization axis was oriented normal to the electron scattering plane [Pow-70]. If time reversal invariance holds, then for elastic scattering this observable is equivalent to the recoil polarization measurements previously discussed to all orders in perturbation theory. The measurements were performed at very forward scattering angles, θ_e between 2.37 and 3.21° at beam energies of 15 and 18 GeV. Data at three momentum transfers, $Q^2 = 0.38$, 0.59 and 0.98 $(\mathrm{GeV/c})^2$ were obtained. The measured quantity is the count rate asymmetry, ϵ_n, between scattering with the target polarized up and down:

$$\epsilon_n = \frac{N_\uparrow - N_\downarrow}{N_\uparrow + N_\downarrow}, \tag{1}$$

where $N_\uparrow$ is the charge normalized number of spectrometer counts with the target polarized

up and $N_\downarrow$ is the analogous quantity with the target polarization down. Their statistically best result was $A_n = -0.005 \pm 0.009$ at the middle momentum transfer [Pow-70]. A_n is the physics asymmetry which is related to the count rate asymmetry, ϵ_n, by

$$A_n = \frac{\sigma_\uparrow - \sigma_\downarrow}{\sigma_\uparrow + \sigma_\downarrow} = \frac{\epsilon_n}{P_T df}. \tag{2}$$

Here P_T is the target polarization and df is the dilution factor. The dilution factor is the ratio of polarized active nucleons to unpolarized active nucleons and is reaction dependent. In the SLAC elastic scattering measurements the target polarization was typically 0.2 and the dilution factor was also about 0.2. Thus a 0.04% count rate asymmetry would correspond to a physics asymmetry of 1%. The normal polarization is given by

$$P_n = A_n = 2i\frac{TrM_1(\sigma \cdot s)ImM_2}{TrM_1M_1}, \tag{3}$$

where M_1 is the one-photon exchange amplitude and M_2 is the two-photon contribution. Unitarity implies that

$$Im < ep|M_2|ep >= \sum_N < ep|T^+|N >< N|T|ep >, \tag{4}$$

with $< N|T|ep >$ being the inelastic electron proton scattering amplitude in the one-photon exchange approximation. Guerin and Piketty estimated the polarization in a model that approximates the dispersive sum by its contributions from the proton, and the first two resonances. Their results indicate that P_n is of order 10^{-3} for electron energies of 1 GeV or less at moderate e-p center of mass angles (the polarization vanishes at $\theta_{cm} = 0$) [Gue-64] as shown in Figure 4. Thus none of the existing measurements is sensitive to the predicted scale of the effect. The existing world data for both P_n and A_n in elastic e-p scattering is shown in figure 5.

Rock et al. tried to measure an asymmetry in inelastic scattering as part of the same experiment as Powell [Roc-70]. They used the same beam energies and forward angles but looked at resonance excitation. This experiment was intended as a test of time reversal invariance, TRI. For elastic scattering from a spin-$\frac{1}{2}$ target, A_n must be zero in first Born approximation as a consequence of gauge invariance, hence any effect must be due to higher order diagrams. This is not the case for inelastic transitions for which a TRI odd current could contribute in first order. Results were quoted for three values of invariant mass, W, corresponding to excitation of the $\Delta(1236)$, $N^*(1512)$ and the $N^*(1688)$. For each W three

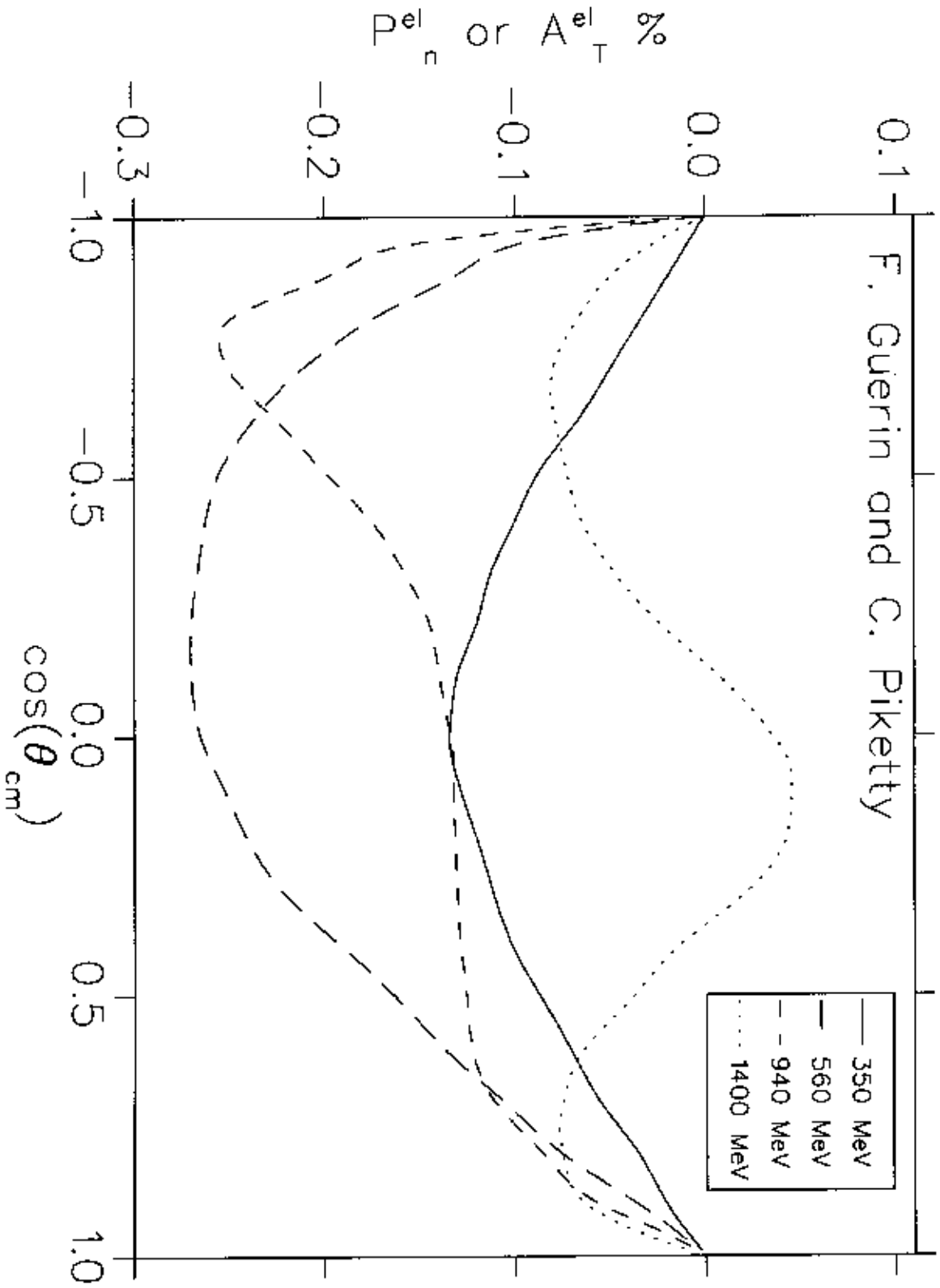

Figure 4: The polarization P_n as a function of θ_{cm} for different incident beam energies [Gue-64].

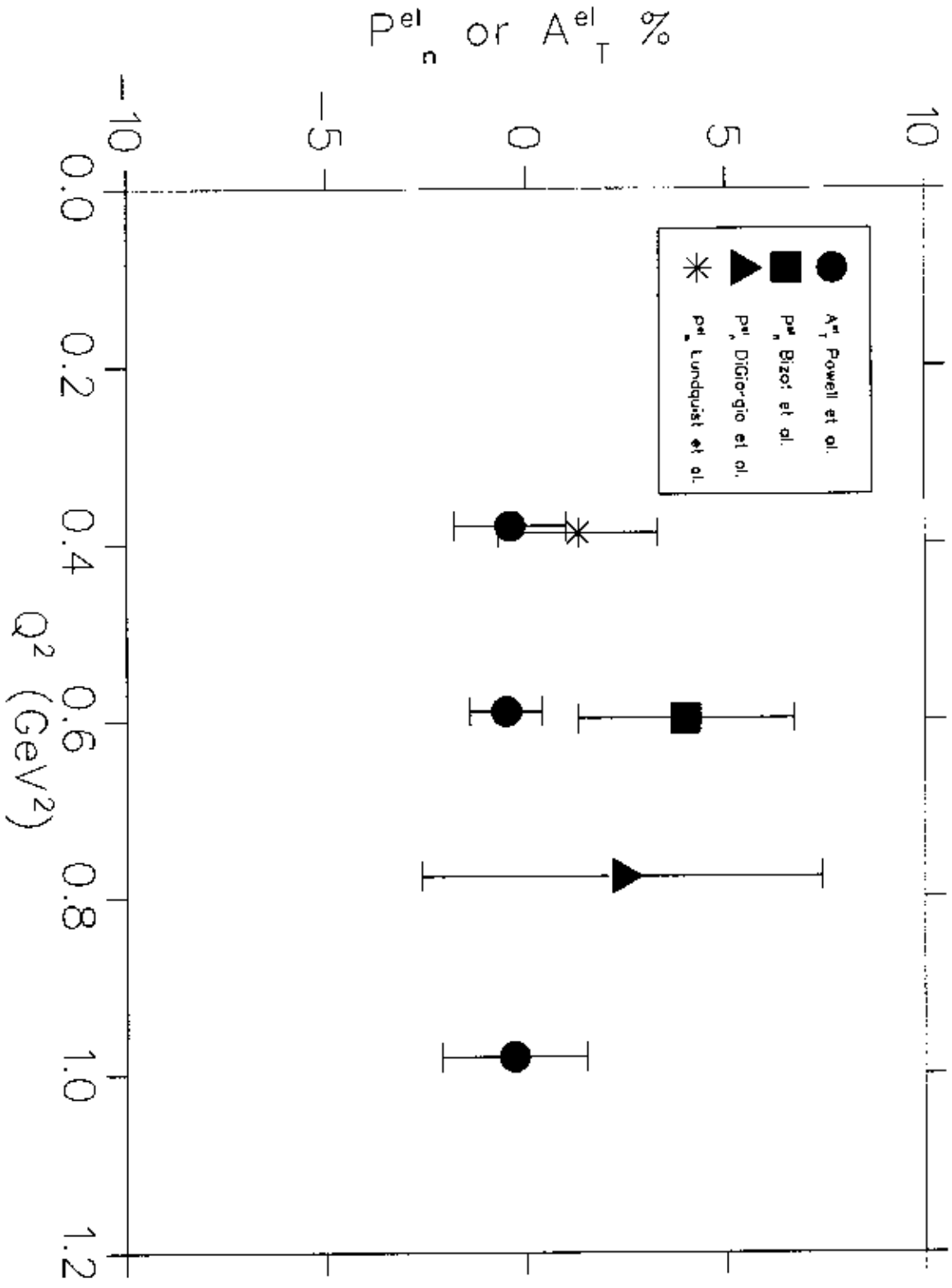

Figure 5: The existing world data for both P_n and A_n in elastic e-p scattering.

values of Q^2 were measured, 0.4, 0.58 and 0.96 $(GeV/c)^2$. In order to separate possible TRI odd effects from two-photon effects, measurements of A_n were made with both electrons and positrons at the lowest Q^2 value in the region of the Δ. Any TRI odd effect would not change sign between e^- and e^+ scattering while the sign of a dispersive contribution would reverse.

Although one of their individual data points is two sigma from zero the data show no consistent deviation from zero. The authors conclude that their results are consistent with zero effect. Their best statistical value is for the asymmetry near the $\Delta(1236)$ at $Q^2 = 0.58\,(GeV/c)^2$. For these conditions they report $A_n = 0.028 \pm 0.014$. An earlier polarized target measurement by Chen et al. [Che-68] found A_n consistent with zero but with statistical errors of 4 to 8%. A sample of the data from these experiments is shown in Figure 6. Cahn and Tsai calculated the two-photon contribution to A_n for the kinematics of the Rock experiment, $E_0 = 18$ GeV and $Q^2 = 0.6\,(GeV/c)^2$. They examined all the two-photon diagrams with a Δ in the final state but approximated the dispersive sum with only the contribution from the proton. They found $A_n = 0.0075$ in the inelastic region with little sensitivity to W in their model [Cah-70].

In summary, despite many years of extensive effort the only data that exhibit a clear, unambiguous signature of dispersive effects is that for the "filling in of the minimum in the elastic form factor of carbon". The observed effect in these data is large and is due to the imaginary part of the dispersive amplitude.

For the nucleon, the measurements of R indicate that the real part of the dispersive amplitude is small, less than 0.3% of the Born term in the kinematics studied. No measurements using polarization techniques have been made with sensitivity to the anticipated size of the asymmetry which is of order 10^{-3}. In fact, the present limits on the size of the spin dependent imaginary piece of the dispersive amplitude are about one order of magnitude greater than this scale, 1%.

3 Proposed Experiment

We propose to measure A_n for the elastic, and quasi-elastic scattering of unpolarized electrons from a polarized ^{3}He target. ^{3}He is an ideal target for these studies for a number of reasons.

- Elastic scattering from ^{3}He offers a chance to measure the dispersive effect in a simple nuclear system where calculations should be more

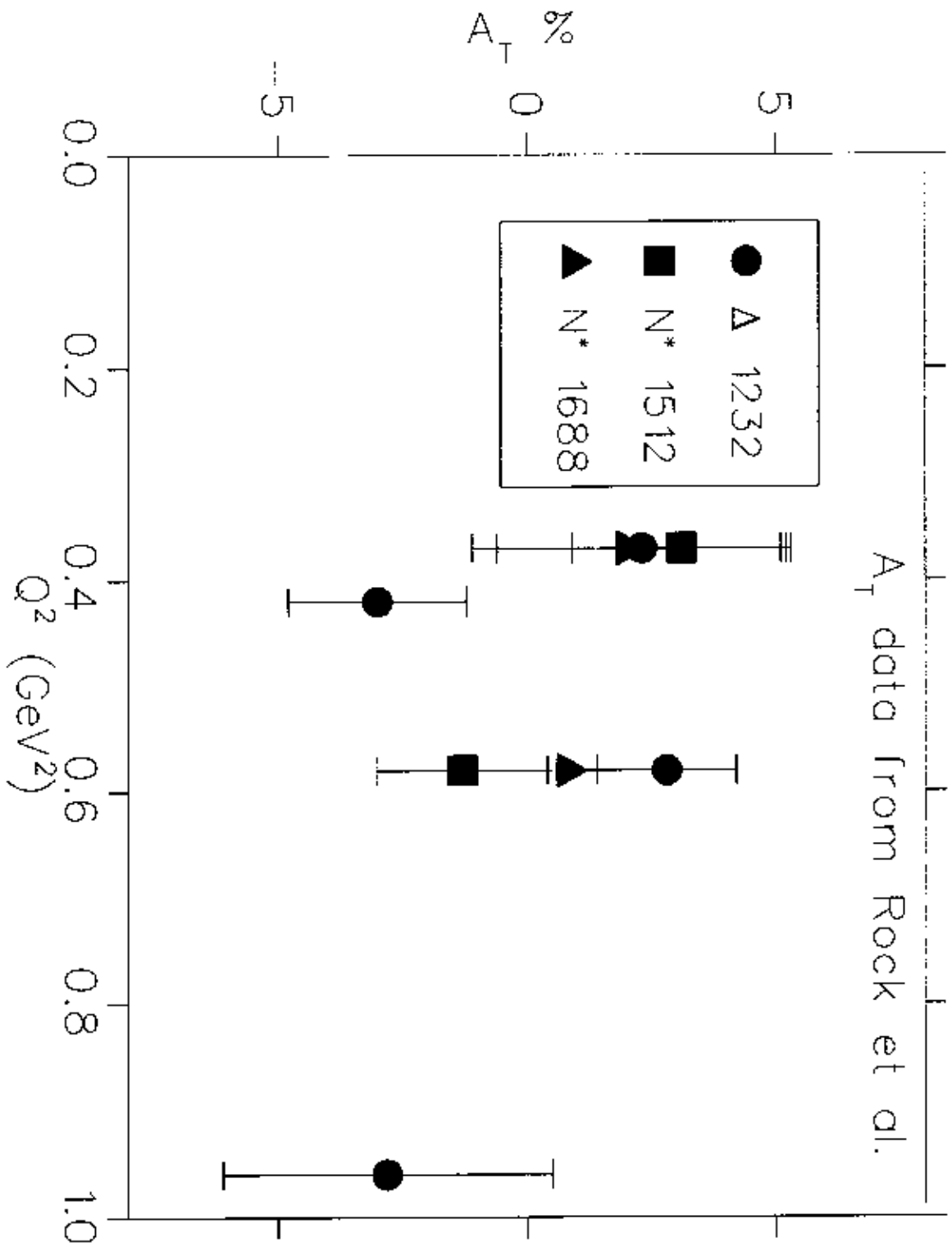

Figure 6: Data for the polarized target asymmetries measured in inclusive resonance electroproduction.

tractable than in the case of ^{12}C. The past years have shown considerable progress in calculational techniques for the static properties of the ^{3}He nucleus, its response to electromagnetic probes, and the relativistic treatment of the 3-nucleon dynamics. Faddeev equations have been solved both in coordinate [Che-85] and momentum [Sas-83] representations. These techniques have been expanded to also calculate dynamic properties [Gol-95]. Alternatively, numerical methods have been developed, either by expansion of the three-nucleon wave function in a Harmonic-Hyperspherical basis [Kie-93] or by using variational non-relativistic Green's-Function Monte Carlo techniques [Car-91], [Wir-91]. Recently, the addition of relativistic effects to the latter has been considered [For-95]. Methods have also been developed [Mar-95], where the 3-body response function is obtained by the inversion of a calculation of its Lorentz-transform. Many of these methods give essentially exact calculations of the inclusive response function of the ^{3}He nucleus. There are few systems for which the theoretical machinery is so well developed.

- Quasi-elastic scattering provides a chance to get a more precise look at dispersion in the "nucleon". This is a fundamental quantity, an imaginary part of a "polarizability". Much theoretical and experimental effort has been devoted lately to investigate the nucleon's response to a static electromagnetic field in terms of its polarizabilities. In electron scattering, a virtual photon may excite a nucleon, which in its turn may de-excite through emission of a real (bremsstrahlung) photon. Experimentally, it is hard to pinpoint this process due to the large background of events where one of the relativistic electrons emitted a similar real photon, but several experimental programs are underway. Theoretically, generalized polarizabilities have been defined for such a Virtual Compton Scattering process by Guichon et al. [Gui-95] Lately, calculations of these generalized polarizabilities have been attempted in diquark models [Kro-96], the linear σ model [Dre-97], effective Lagrangian models [Van-96], [Sch-97] and in the framework of Chiral Per-

turbation Theory [Hol-97]. Of interest for this experiment is that the asymmetry we measure for the quasi-elastic electron-nucleus process is essentially sensitive to the same diagram the Virtual Compton Scattering process is, with one caveat: in the Virtual Compton Scattering process the virtual photon fixes the momentum transfer Q^2, while in the two-photon exchange process the momentum transfer Q^2 is shared by two virtual photons, requiring an integration over the shared momentum in the calculations.

- Experimentally, ^{3}He targets require only a weak, 20 to 40 Gauss holding field. This means that no correcting chicane is needed and greatly simplifies the experimental installation. After a successful quasi-elastic helium measurement is complete the more complicated proton experiment could be attempted (there have been great improvements in polarized proton targets since the 1970's).

4 Experimental Method

The proposed experiment will be carried out in Hall A using the High Resolution Spectrometers (HRS) and a polarized ^{3}He target, with polarization perpendicular to the scattering plane. The scattered electrons from $^3\vec{\text{He}}$(e,e') elastic and quasi-elastic channels will be detected in the HRS. The experimental asymmetry, ϵ_n, is determined from the normalized numbers of scattered electrons detected for target polarization up, $N_\uparrow$, and target polarization down, $N_\downarrow$ (see Equation 1). The physics asymmetry is obtained from the experimental asymmetry, ϵ_n, the target polarization, P_T, and the dilution factor, df (Equation 2). A spin-exchange $^3\vec{\text{He}}$ target will be used in this project. We gain factors of 200 to 100 in sensitivity compared to previous SLAC experiments [Pow-70] in the elastic and the quasi-elastic channels. The polarization will be continuously monitored during the entire experiment. To obtain the desired statistical accuracy in a reasonable running time, the rates will be integrated at the focal plane using a series of scintillator paddles. In the following, we give a detailed description of the experimental technique.

4.1 Target

Two popular techniques have been used for producing polarized ^{3}He for external targets: the metastability exchange method and the spin exchange method by optically pumped alkali-metal vapor. In either case, the target is divided into two cells, the pumping cell and the target cell itself where the beam passes through.

In spin exchange targets, the pumping cell contains a mixture of Rb metal, ^{3}He and nitrogen maintained at a higher temperature (170 – 200 °C) to control the Rb vapor density. The nitrogen increases the efficiency of the optical pumping. The target cell is connected to the pumping cell via a narrow tube and it is maintained at a much lower temperature (50 °C). Polarized ^{3}He nuclei diffuse from the pumping cell to the target cell. The rubidium number density in the target cell is several orders of magnitude less than in the pumping cell where the rubidium is confined by temperature gradient [Chu-94]. The polarization of the ^{3}He nuclei is done in two stages. First, the Rb is polarized by illuminating it with circularly polarized laser light tuned to the Rb D1 line (795 nm). The D1 transition results in the spin polarization of the Rb valence electrons. The second stage of the process involves polarization transfer to the ^{3}He by binary Rb $-^3$ He collisions during which hyperfine interactions between the Rb valence electrons and the ^{3}He nucleus may cause the latter to flip. Since the polarization transfer cross section is very small, the ^{3}He nuclear polarization build-up can take quite a long time [Mid-94]. The primary advantage of the spin exchange polarization targets is the higher target densities — optical pumping in these targets can be performed at higher pressure ($\sim$ 10 atmosphere) in contrast to targets based on metastability exchange method where the pressure is limited to few Torr. We plan to use the Hall A spin exchange target which is being set-up for several approved experiments.

4.2 Polarization and Dilution Measurements

Two methods have been used in electron scattering for ^{3}He target polarization measurements. The NMR technique of adiabatic fast passage (NMR-AFP) has been used for all targets: RF coils produce an oscillating field perpendicular to the main field which is swept through a resonance due to Larmor spin precession. This causes the ^{3}He spin to flip producing a signal in the pick-up coils. The signal intensity is proportional to the target polarization. The system is calibrated with protons from a water sample, with a known thermal polarization of $\sim 10^{-8}$. This method is reliable to a few percent.

Table 1: Target parameters for the proposed experiment.

Density	$2.5\,10^{20}\mathrm{cm}^{-3}$
Length	25 cm
Peak Polarization	40% to 45%
Average Polarization	35%
Dilution Factor (Elastic)	~ 0.75
Dilution Factor (Quasi-elastic)	~ 0.25
Material	^{3}He
Target Holding Field	20 G
Polarization Measurement	NMR-AFP (EPR)

The target polarization will be measured periodically during the experiment by the NMR-AFP technique. It is possible to cross-check the polarization measurements with the Electron Paramagnetic Resonance (EPR) method which consists of measuring the frequency shifts induced by the polarized ^{3}He nuclei on Rb atoms [Rom-97]. The NMR-AFP and the EPR techniques are integral parts of the Hall A polarized ^{3}He target system.

The dilution of the measured asymmetry is due to impurities, or processes involving materials other than ^{3}He, namely beam halo scatterings from target walls and most importantly from the nitrogen buffer gas. Potentially, the rubidium atoms used in the polarization process can also contribute to the dilution. However, the residual rubidium in the target cell has a number density many orders of magnitudes [Mid-94] less than the ^{3}He number density, while the Rb(e,e) cross sections are higher than the ^{3}He(e,e) cross sections by only a factor of ten at the proposed kinematics.

In the kinematics used for the elastic measurements we estimate that scattering from the buffer gas and other unpolarized materials will account for 25 percent of the scatterings. In quasi-elastic kinematics the effect is approximately three times worse as only one of the nucleons in ^{3}He is polarized.

Direct measurements of the the cell wall contribution to the dilution factor will be made periodically during the experiment with empty target cells. Table 1 summarizes the target parameters [Che-98].

4.3 Polarization Reversal

Systematic effects associated with small fluctuations in detector efficiencies, drifts in beam current monitors, changes in beam conditions must be averaged out to be sensitive to asymmetries of order 10^{-4}. We plan to reverse the target polarization once every minute using pulsed NMR techniques. The reversal process is essentially the same as in the normal AFP method with the exception that the RF frequency — not the field — is swept through the resonance [Rom-97]. The advantage is that the holding field remains locked throughout the entire experiment so that the experiment does not build-in a false asymmetry resulting from the reversal of polarization by reversal of the holding field. However, during half of the reversal cycle, the laser will be pumping in the opposite direction and polarization decay will become the major loss of polarization, especially in the presence of beam. This problem is solved by reversing the circular polarization of the laser following each half cycle of the frequency sweep AFP process. In doing so, the only loss of polarization comes from AFP losses which could be kept at the 0.1 to 0.2% level (fractional loss per sweep) by optimizing the sweep rate.

Frequent reversals by this method will decrease the average polarization of the target. One can treat the AFP losses as an extra relaxation mechanism and include it in the relaxation rate equations. On the basis of such a calculation we estimate that the reversal losses will decrease the average polarization by about 5 percent and hence a target polarization of 35 percent has been used in all error and run time estimates.

4.4 Rates

The rates for elastic scatterings are estimated based on the following:

$$R = \mathcal{L}\frac{d\sigma}{d\Omega}\Delta\Omega, \tag{5}$$

where

$$\frac{d\sigma}{d\Omega} = \frac{1}{f}\frac{d\sigma}{d\Omega_o}\left(A(Q^2) + B(Q^2)\tan^2(\theta/2)\right). \tag{6}$$

$\frac{d\sigma}{d\Omega_o}$ is the Mott cross section, f is the recoil factor, and $A(Q^2)$ and $B(Q^2)$ are the elastic form factors of ^{3}He, θ is the electron scattering angle in the lab, and $\Delta\Omega$ is the solid angle acceptance of the spectrometer. For the quasi-elastic measurements, the rates are calculated from

$$R = \mathcal{L}\frac{d^2\sigma}{d\Omega\, dE'}\Delta\Omega\Delta\, E' \tag{7}$$

where ΔE is the energy bin. In our estimation of the rates, we assumed $\Delta\Omega = 6\,\mathrm{msr}$, $\Delta E = 4\%\,E'$, a beam current of $15\,\mu$A and the target parameters of Table 1. The elastic and the quasi-elastic measurements will be carried out concurrently by using both spectrometers, one for the elastic and the other for the quasi-elastic processes. Tables 2 and 3 show the kinematics of the proposed experiment and the estimated rates. The kinematics were chosen so that the higher momentum transfer would be comparable to the momentum transfer at the ^{12}C minimum where large dispersive effects have been observed. This is still small enough to allow the gathering of very high statistics in a reasonable time. Two points will be measued to check the beam energy or momentum transfer dependence. At our angles, background events coming from the target windows will not be accepted in the spectrometers. Therefore, no collimation will be necessary to remove these events. The statistical uncertainty in the

Table 2: Kinematics and rates for the elastic channel.

Beam Energy (GeV)	0.845	1.645
Spectrometer angle (deg.)	17.0	12.5
Q^2 (fm^{-2})	1.58	3.25
Scattered Energy (GeV)	0.840	1.622
Rate (kHz)	29.0	5.0

Table 3: Kinematics and rates for the quasi-elastic channel.

Beam Energy (GeV)	0.845	1.645
Spectrometer angle (deg.)	17.0	12.5
Q^2 (fm^{-2})	1.54	3.14
Scattered Energy (GeV)	0.810	1.570
W (GeV)	0.943	0.950
Rate (kHz)	48.7	37.4

experimental asymmetry (Equation 1) is

$$\delta\epsilon_n \simeq \frac{1}{\sqrt{N}}, \tag{8}$$

where N is the total number of counts for target polarization up or down. Combining Equations 2 and 8, we have

$$N = \frac{1}{(df\ P_T \delta A_n)^2} = Rt, \tag{9}$$

where δA_n is the statistical error on the physics asymmetry, R is the rate and t is the acquisition time.

4.5 Data Acquisition and Detectors

The rates quoted in Table 2 and Table 3 are higher than the maximum rate of the standard data acquisition (DAQ) in Hall A.

We will integrate the rates using segmented plastic scintillator detectors at the focal plane (for the elastic channel), shower counter blocks (for the quasi-elastic channel) and STRUCK scalers STR7201.

Monte Carlo simulation has shown that elastic events can be separated partially at the focal plane from the quasi-elastic continuum for the kinematic conditions of this experiment. Figure 7 shows the result of the simulation. Here, we show the separation between the elastic and the break-up events for 1-pass and 2-pass beams and the HRS at 12.5 and 17.0 degrees. The design of the scintillator paddles is based on this result. We will install nine paddles of 1.5 cm wide, 20 cm long and readout at both ends. A schematic layout of the scintillators is shown in Figure 8. If need be, we can change the (x,x') focus to get it "straight" on the paddles.

The expected experimental asymmetry ϵ_n is of the order 10^{-4}; to reduce the systematics below the statistical uncertainties (Table 4), it is necessary to avoid any false asymmetry inherent to the readout process itself. Therefore, the timing and the readout cycle of the scalers are critical.

The STR7201 is a 32-bit, 32-channel scaler with input rate up to 200 MHz. The scaler is equipped with two independent data banks and a FIFO designed to minimize readout overheads and in doing so, to provide essentially continuous counting. A clock triggers the change of the active data bank. Counting is disabled for 10 ns to complete the change, the data in the inactive bank is latched onto the FIFO and the inactive bank is cleared while counting has resumed for the active bank. The FIFO readout overhead is only 4 μs. The situation is depicted in Figure 9.

A 32-bit scaler can handle a 1 MHz rate for 70 Minutes without turning over. We plan to

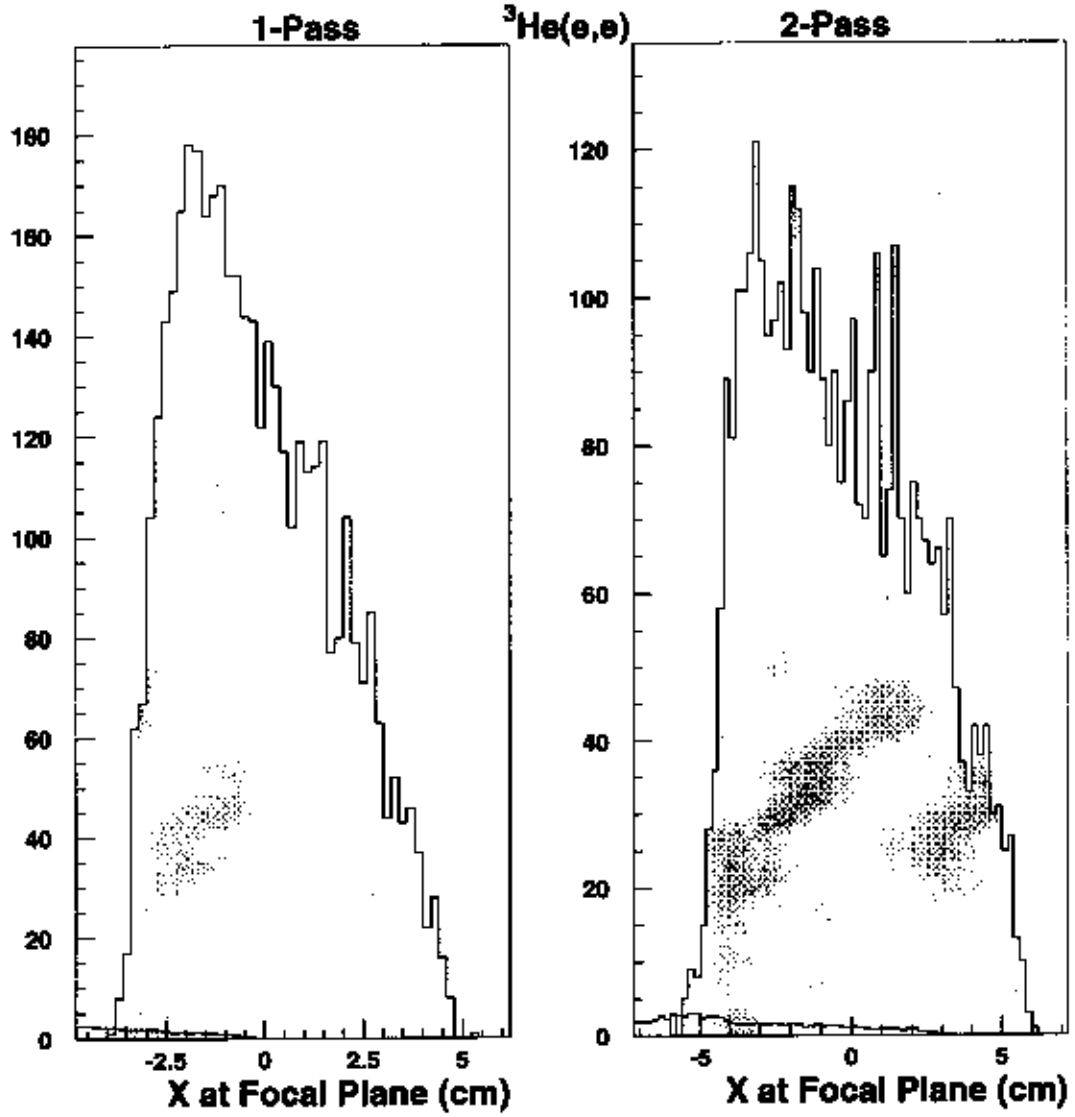

Figure 7: Separation of elastic and break-up (5.5 MeV) events at the focal plane for 1- and 2-pass settings. The shaded spectra correspond to elastic channel and the unshaded ones to break-up channel. The normalizations are given by the cross sections ratios.

push the FIFO approximately once every 10 seconds. This will allow relatively easy checks of the system stability: at 10 kHz one gets 0.3 % statistics in 10 seconds. In addition, the scaling of a one MHz clock will allow additional checks to be performed off-line. The FIFO readout will be synchronized with the target polarization reversal.

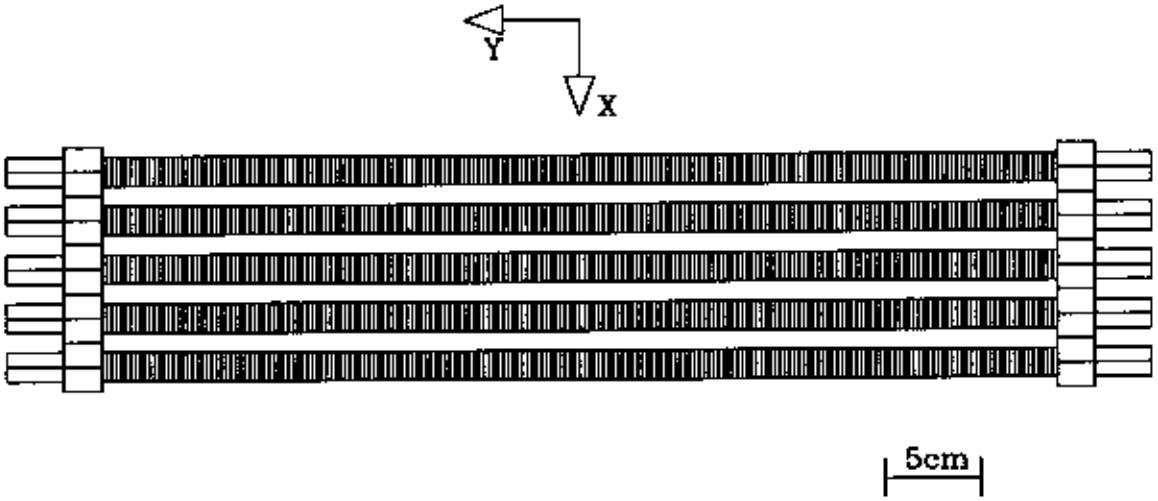

Figure 8: Schematic Layout of the scintillator paddles to be installed at the focal plan for the elastic $^3\vec{H}e(e,e')$. The scintillators are viewed at both ends. Only five of the paddles are shown here for clarity. The rest is interleaved between the ones shown.

At the maximum expected rate of 50 kHz, with 50 ns pulse widths, the discriminator and scaler dead-times are about 3 ppm and hence even if uncorrected are smaller than our expected asymmetries. The dead-time associated with pushing the FIFO and reading the FIFO are both completely negligible. A pulser system will be used to check the electronics dead-time.

We will also use the standard DAQ in short dedicated runs to monitor changes in the beam and the focus, and to estimate the small fractions of the quasi-elastic continuum under the elastic spectra (Figure 7). The normal configuration of the HRS will be in place, i.e., there will be particle identification behind the scintillator paddles.

4.6 Systematic Uncertainties

Systematic uncertainties associated with detector efficiencies and solid angle will cancel in the ratio for the asymmetry measurements. Fluctuations in detector efficiencies, drifts and changes in beam conditions will be averaged out by the polarization reversal cycles. However, systematic uncertainties related to the target polarization state will not cancel in the ratio. The major source of systematics will come from the target polarization measurements. The polarization will be measured periodically during the experiment with the NMR-AFP

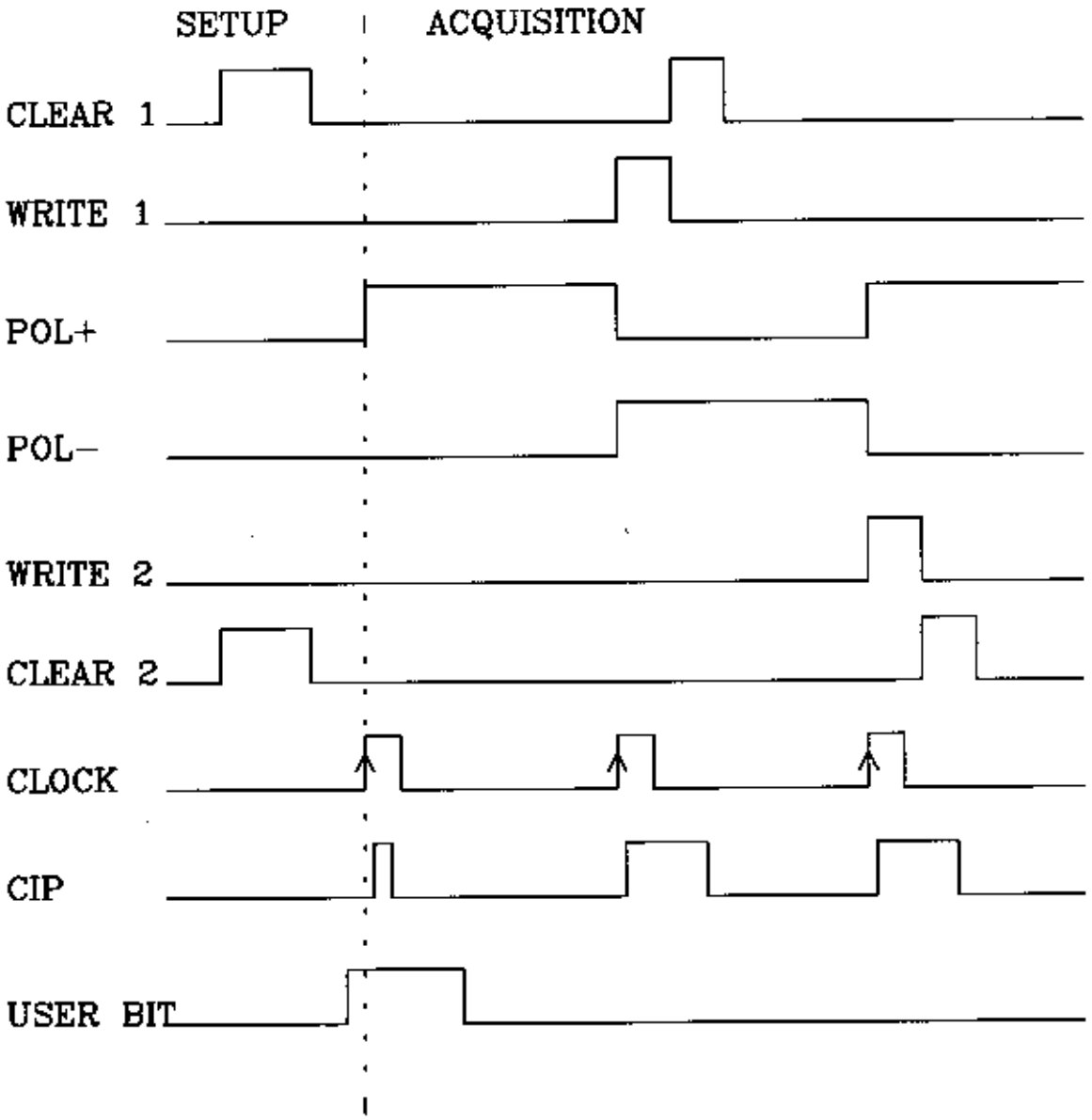

Figure 9: The readout consists of switching counting to the inactive data bank and latching the data in the previously active bank to the FIFO. Counting is inhibited during the 10 ns needed to complete the switch. CIP (Copy In Progress) is asserted while data is being copied to the FIFO. During that time, clock transitions are inhibited. A FIFO half full signal triggers the readout of the FIFO itself during next polarization reversal.

technique and cross-checks will made with the EPR method.

In order to check for false asymmetries we will perform high statistics measurements on an unpolarized target.

5 Beam Time Request

We plan to measure the physics asymmetry at two Q^2 settings for both the elastic and the quasi-elastic channels. The beam time requested is shown in Table 4 along with the

Table 4: Beam time requirement for the proposed experiment. The **'s indicate simultaneous measurements with the corresponding elastic settings.

	δA_n	Time (days)
Physics Asymmetry (Elastic, 1-pass)	0.4×10^{-4}	4
Unpolarized Target (Elastic, 1-pass)	0.2×10^{-4}	1
Physics Asymmetry (Quasi-elastic, 1-pass)	1.0×10^{-4}	**
Physics Asymmetry (Elastic, 2-pass)	1.0×10^{-4}	4
Unpolarized Target (Elastic, 2-pass)	0.5×10^{-4}	1
Physics Asymmetry (Quasi-elastic, 2-pass)	1.0×10^{-4}	**
Dilution Effects		2
Checkout, Calibration		1
Configuration Change		1
Total		14

expected statistical uncertainties on the physics asymmetries. We request a total of 14 days for a measurement of the elastic asymmetry at 1-pass down to the 4×10^{-5} level, and down to the 1×10^{-4} level at other settings. The requested time includes all the overhead due to calibration, polarization measurements and reversals, and momentum, beam and angle changes.

The unpolarized target measurements constitute a systematic check of the proposed experimental method since the asymmetry must vanish in the absence of target polarization.

6 Conclusion

We propose to measure the physics asymmetries in inclusive elastic and quasi-elastic $^3\vec{\mathrm{H}}\mathrm{e}(\mathrm{e},\mathrm{e}')$ scatterings. Non-vanishing asymmetries can only result from dispersive or multi-photon exchange processes (elastic and quasi-elastic channels), or time reversal invariance violation

(quasi-elastic channel only). Previous measurements with polarization techniques are not sensitive to the expected size of these effects, i.e., $\sim$ 0.1% [Gue-64],[Cah-70]. We propose to measure these effects with a statistical accuracy of $\sim$ 0.004% using the high resolution spectrometer and the spin exchange polarized ^{3}He target of Hall A. The only new equipment needed are the scintillators for the elastic measurement. This experiment is a factor of 200 more sensitive than the previous best measurement of a dispersive spin observable !

Most systematic effects will be eliminated by appropriate polarization reversal cycles. To achieve the proposed statistical accuracy in the requested beam time period, we plan to integrate the rates using an array of plastic scintillator paddles (at the focal plane) and the shower counter blocks. We will use the standard Hall A data acquisition system and beamline instrumentation to monitor changes in the beam and detector conditions.

References

[Abr-61] *Principle of Nuclear Magnetism*, A. Abragham (London: Oxford University Press 1961), pp 599

[And-68] R.L. Anderson, et al., Phys. Rev. **166**, 166 (1968)

[Bar-67] W. Bartel, et al., Phys. Rev. Lett. **25B**, 242 (1967)

[Bar-60] A.O. Barut and C. Fronsdal, Phys. Rev.**120**, 1871 (1960)

[Biz-65] J.C. Bizot, et al., Phys. Rev. **140**, 1387 (1965)

[Boq-68] B. Bouquet, et al., Phys. Lett. **26B**, 178 (1968)

[Bor-71] E. Borie and D. Drechsel, Phys. Rev. Lett. **26**, 195 (1971)

[Bre-91] V. Breton, et al., Phys. Rev. Lett. **66**, 572 (1991)

[Bro-64] A. Browman, et al., Phys. Rev. **139**, 1079 (1965)

[Cah-70] R. Cahn and Y.S. Tsai, Phys. Rev. D **2**, 870 (1970)

[Car-91] J. Carlson, in *Structure of Hadrons and Nuclear Matter*, eds. O. Scholten and J.H. Koch, World Scientific (1991) 43.

[Cas-67] G. Cassiday, et al., Phys. Rev. Lett. **19**, 1191 (1967)

[Che-98] J.P. Chen, The GDH Sum Rule and the Spin Structure of ^{3}He and the Neutron using Nearly Real Photons, Proposal submitted to JLab PAC 13.

[Che-85] C.R. Chen, G.L. Payne, J.L. Friar, and B.F. Gibson, Phys. Rev. C **31** (1985) 266.

[Che-68] J.R. Chen, et al., Phys. Rev. Lett. **21**, 1279 (1968)

[Chu-94] T. .E. Chupp, R. J. Holt, R .G. Milner, Optically Pumped Polarized Gaseous H,D and^{3}He Gas Targets, Annual Reviews of Nuclear and Particle Science, **44**, (1994) 373

[DiG-65] G.V. Di Giorgio, et al., Il Nuovo Cimento **39**, 474 (1965)

[Dre-97] A. Metz and D. Drechsel, nucl-th/9607050; D. Drechsel, G. Knochlein, A. Metz, and S. Scherer, Phys. Rev. C **55** (1997) 424.

[Dre-58] S.D. Drell and S. Fubini, Phys. Rev. **113**, 741 (1959)

[Fan-76] D.L. Fancher, et al., Phys. Rev. Lett. **37**, 1323 (1976)

[For-95] J.L. Forest, V.R. Pandharipande, and J.L Friar, Phys. Rev. C bf 52 (1995) 568.

[FrR-74] J.L. Friar and M. Rosen, Ann. Phys. **87**, 289 (1974)

[Gen-93] T. R. Gentile, R. D. McKeown, Phys. Rev. A **47**, 456 (1993)

[Gue-64] F. Guerin and C.A. Piketty, Il Nuovo Cimento**32**, 971 (1964)

[Gui-95] P.A.M. Guichon, G.Q. Liu, and A.W. Thomas, Nucl. Phys. **A591** (1995) 606.

[Gol-95] J. Golak *et al.*, Phys. Rev. C **51** (1995) 1638; **52** (1995) 1216.

[Han-95] J. Hansen, PhD Thesis, Massachusetts Institute of Technology, 1995

[Hei-94] W. Heil, AIP Conf. Proc., **293**, 239 (1994)

[Her-97] T. Herrmann and R. Rosenfelder, PSI preprint (1997)

[Hol-97] T.R. Hemmert, B.R. Holstein, G. Knochlein, and S. Scherer, Phys. Rev. D **55** (1997) 2630.

[Jos-74] H. Jostlein, et al., Phys. Lett. **52B**, 485 (1974)

[Kie-93] A. Kievsky, M. Viviani, and S. Rosati, Nucl. Phys. **A551** (1993) 241; **A577** (1994) 511;

[Kla-86] S. Klarsfeld et al., Nucl. Phys. **A456**, 373 (1986)

[Kro-96] P. Kroll, M. Schřmann, and P.A.M. Guichon, Nucl. Phys. **A598** (1996) 435.

[LeD-94] M. LeDuc et al., AIP Conf. Proc. **293**, 499 (1994)

[Lor-93] W. Lorenzon et al., Phys. Rev. A **47**, (1993) 468

[Lun-68] D.E. Lundquist, et al., Phys. Rev. **168**, 1527 (1968)

[Mar-95] S. Martinelli, H. Kamada, G. Orlandini, and W. Glockle, Phys. Rev. C **52** (1995) 1778.

[Mar-68] J. Mar, et al., Phys. Rev. Lett. **21**, 482 (1968)

[Mid-94] H. Middleton et al, AIP Conf. Proc., **293**, 244 (1994); *The Spin Structure of the Neutron Determined Using Polarized* ^{3}*He Target* by Hunter Leigh Middleton, Princeton University, 1994.

[Mil-89] R. G. Milner, R. D. McKeown, C. E. Woodward, Nucl. Inst. Meth. **A274**, 56, (1989)

[Off-91] E.A.J.M. Offermann, et al., Phys. Rev. C **44**, 1096 (1991)

[Pac-94] K. Pachucki et al., Phys. Rev. A **49**, 2255 (1994)

[Pow-70] T. Powell, et al., Phys. Rev. Lett. **24**, 753 (1970)

[Pre-68] R. Prepost, R.M. Simonds and B.H. Wilk, Phys. Rev. Lett **21**, 1271 (1968)

[Roc-76] L.S. Rochester, et al., Phys. Rev. Lett. **36**, 1284 (1976)

[Roc-70] S. Rock, et al., Phys. Rev. Lett. **24**, 748 (1970)

[Rom-97] *Laser Polarized ^{3}He Target used for a Precision Measurement of the Neutron Spin Structure* by Mikhail Romalis, Princeton University, 1997.

[Sas-83] T. Sasakawa and S. Ishikawa, Few-Body Syst. **1** (1983).

[Sch-93] F. Schmidt-Kaler et al., Phys. Rev. Lett. **70**, 2261 (1993)

[Sch-97] A.Yu. Korchin and O. Scholten, in Conf. Handbook of XVth Int. Conf. on Few-Body Problems in Physics, Groningen, 1997, eds. L.P. Kok, J.C.S. Bacelar, and A.E.L. Dieperink.

[Sic-96] I. Sick and D. Trautmann, Phys Lett **B375**, 16 (1996)

[Tho-92] A. K. Thompson, Phys. Rev. Lett. **68**, 2901 (1992)

[Tim-71] R. S. Timsit, J. M. Daniels, A. D. May, Can. J. Phys., **49**, 560 (1971)

[Van-96] M. Vanderhaeghen, Phys. Lett. **B368** (1996) 13.

[Voe-91] N. Voegler, et al., Phys. Rev. C **43**, 2172 (1991)

[Wir-91] R.B. Wiringa, Phys. Rev. C **43** (1991) 1585.

[Woo-90] C. E. Woodward et al., Phy. Rev. Lett. **65**, 698 (1990)

[You-62] D. Yount and J. Pine, Phys. Rev. **128**, 1842 (1962)